

Papillation in *Bacillus anthracis* colonies: a tool for finding new mutators

Hanjing Yang,¹ Cameron Sikavi,¹ Katherine Tran,¹ Shauna M. McGillivray,² Victor Nizet,³ Madeline Yung,¹ Aileen Chang¹ and Jeffrey H. Miller^{1*}

¹Department of Microbiology, Immunology, and Molecular Genetics, Molecular Biology Institute, University of California, David Geffen School of Medicine, Los Angeles, CA 90095, USA.

²Department of Biology, Texas Christian University, Fort Worth, TX 76129, USA.

³Division of Pediatric Pharmacology & Drug Discovery, UCSD School of Medicine, Skaggs School of Pharmacy and Pharmaceutical Sciences, La Jolla, CA 92093, USA.

Summary

Colonies of *Bacillus anthracis* Sterne allow the growth of papillation after 6 days of incubation at 30°C on Luria–Bertani medium. The papillae are due to mutations that allow the cells to overcome the barriers to continued growth. Cells isolated from papillae display two distinct gross phenotypes (group A and group B). We determined that group A mutants have mutations in the *nprR* gene including frameshifts, deletions, duplications and base substitutions. We used papillation as a tool for finding new mutators as the mutators generate elevated levels of papillation. We discovered that disruption of *yycJ* or *recJ* leads to a spontaneous mutator phenotype. We defined the *nprR*/papillation system as a new mutational analysis system for *B. anthracis*. The mutational specificity of the new mutator *yycJ* is similar to that of mismatch repair-deficient strains (MMR⁻) such as those with mutations in *mutL* or *mutS*. Deficiency in *recJ* results in a unique specificity, generating only tandem duplications.

Introduction

The principle of papillation, the phenomenon of producing secondary colonies (or microcolonies) growing out of the

surface of the main colony, has been used for decades in biological processes, and in particular, mutagenesis. Typically, solid agar plates contain two alternative nutrients, one of which can readily be used by a given strain. After using up the first nutrient colonies stop growing, but subsequently papillae appear that contain mutants that are now proficient in utilizing the secondary nutrient. Early work by Massini (1907) demonstrated papillation by *Bacterium coli-mutabile* when plated on lactose indicator agar plates. Unable to ferment lactose, these bacteria formed pale colonies. After some days papillae appeared on the surface of parental colonies, which were now able to ferment lactose, and the acids produced from fermentation coloured the papillae red from the centre outwards in the presence of an indicator such as neutral red (Parr and Thomas, 1942; Dean and Hinshelwood, 1957a,b; and refs therein). Monod utilized this technique to study spontaneous mutations in *Escherichia coli-mutabile* (Monod and Audureau, 1946). Clearly, two factors are required for papillation to occur: one is external, such as the appropriate sugar in the example here, and one internal such as the mutation.

Papillation is a widely used assay in the field of DNA mutagenesis and repair. An example is using the blue papillation assay (Nghiem *et al.*, 1988), often used with a set of *E. coli lacZ* strains constructed to monitor the rates of base substitutions or frameshifts at one specific site of the *lacZ* gene (Cupples and Miller, 1989; Cupples *et al.*, 1990). If mutations occur to revert *lacZ* back to the wild type, blue papillae will form on the surface of white parental colonies on glucose minimal plates containing X-Gal and P-Gal. Correlation between the rate of papillation and the rate of mutation allows one to readily detect mutators that have elevated mutation rates by monitoring the levels of papillae formation (Cabrera *et al.*, 1988; Nghiem *et al.*, 1988; Michaels *et al.*, 1990; Miller, 1996; Miller and Michaels, 1996; Slupska *et al.*, 2000; Miller *et al.*, 2002). Papillation assays have also been successfully used in other areas, such as recombination (Konrad, 1977), adaptive mutagenesis (for reviews, see Foster, 1993; 2007), screening for transformation-deficient mutants (Lacks and Greenberg, 1977) and hyperactive transposase mutants (Lampe *et al.*, 1999), as well as elucidating mechanisms of human activation-induced deaminase expressed in *E. coli* (Wang *et al.*, 2009).

Accepted 15 December, 2010. *For correspondence. E-mail jhmill@microbio.ucla.edu; Tel. (+1) 310 825 8460; Fax (+1) 310 206 3088.

Bacillus anthracis is a Gram-positive spore-forming bacterium. Its life cycle has two stages – vegetative growth and sporulation (for reviews, see Koehler, 2009; Kolstø *et al.*, 2009). In a nutrient-rich environment *B. anthracis* cells rapidly grow and divide. When environmental conditions become unfavourable, the vegetative cells undergo growth arrest and differentiate into endospores that are metabolically dormant and able to survive under extreme conditions for long periods of time. Studies of *Bacillus* and *Myxococcus* developmental networks and their transcriptional regulators have shown that the transition between vegetative growth and sporulation is governed by environmental signals such as nutritional, cell density and cell cycle signals (for review, see Kroos, 2007). Signal transduction pathways in the early onset of sporulation have been extensively studied in *Bacillus subtilis*, where environmental signals activate multiple sensor histidine kinases that in turn activate a key response regulator Spo0A by increasing its phosphorylation level (Perego and Hoch, 2002). Phosphorylated Spo0A initiates a cascade of signal transduction pathways that lead to asymmetric cell division, a hallmark of the onset of sporulation. Similar to *B. subtilis*, the onset of sporulation of *B. anthracis* also triggers programmed transcription of a large set of genes that are distinct from those transcribed during vegetative growth (Bergman *et al.*, 2006; Day *et al.*, 2007).

Papillation has been observed in *B. anthracis*. Early work by Stewart reported that papillae formed on the *B. anthracis* colonies were conspicuously bright and shiny in the presence of transmitted light on the surface of dull and off-white colonies and may look like small air-bubbles (Stewart, 1928). Work by Yabuuchi and Koseki (Yabuuchi and Koseki, 2003) documented that under aerobic condition on 5% sheep blood agar (or chocolate agar), numerous dew-like shiny dots appeared on the surface of *B. anthracis* EY 3169^T (=ATCC 14578^T) colonies after 10 or more days' incubation at room temperature. It has been considered that they are daughter colonies growing out of the parent colony (Stewart, 1928; Yabuuchi and Koseki, 2003). Papillation in *B. subtilis* and *B. anthracis* has also been observed in special cases, where the parental strains are hypersporulating mutants due to mutations in genes that are critical for the sporulation network. Papillae arise as sporulation-deficient mutants (Spiegelman *et al.*, 1990; Perego and Hoch, 1991; Ohlsen *et al.*, 1994; Perego *et al.*, 1994; Bongiorno *et al.*, 2007).

Our goal is to understand the molecular nature of papillation and to develop tools for finding mutators in *B. anthracis*. In this work we report that a main subtype of papillation mutants contains mutations in the *nprR* gene, encoding a DNA transcriptional regulator for extracellular protease production. We also report using papillation as a tool for finding new mutators and identified two new spon-

taneous mutators: *yycJ* and *recJ*. We defined a new *nprR* papillation mutational analysis system and used it to characterize mutational specificities of *yycJ* and *recJ*.

Results

Papillation in wild-type *B. anthracis* colonies

When wild-type *B. anthracis* Sterne colonies were incubated at 30°C for 6 or more days on LB plates, papillae appeared as dew-like shiny dots on the surface of parental colonies. An example is shown in Fig. 1 (Fig. 1A–D). While off-white colonies formed after a 1 day incubation at 30°C (Fig. 1A and C), tiny dots started to appear on the surface of parental colonies on day 4, when observed under a dissection microscope (data not shown); and became prominent to the naked eye on day 6 (Fig. 1B and D). These observations are consistent with previous reports, where these dew-like shiny dots were referred to as daughter colonies (Stewart, 1928; Yabuuchi and Koseki, 2003). The size of the papillae varies. Some are in the range of several hundred micrometers, while others are smaller.

We isolated cells from independent papillae and observed that the colony morphology of these isolates was clearly different from the wild type. An example is shown in Fig. 1E and F, where both a wild type and a papillation mutant were streaked on the same LB plate in a pattern where the colonies overlapped at the centre (Fig. 1E). After a 2 day incubation at 30°C, colonies of the papillation mutant appeared thicker than those of the wild type and had a different light reflection feature (Fig. 1E). They displayed no visible papillae on day 6 (Fig. 1F). Our results indicate that the cells isolated from papillae are mutants that have acquired certain mutations during growth.

Diversity of papillation mutants

We used a 96-well format to display and compare the phenotype of a large group of independent papillation mutants. Specifically, we isolated 243 papillation mutants from the wild-type *B. anthracis*, arrayed them in 96-well plates along with wild-type controls, printed them onto several different types of solid agar plates, and observed the cell patch morphology for an extended period of time. An example is shown in Fig. 2. The plate is arranged with four pairs of wild-type controls (Fig. 2A, cell patches marked with grey brackets: T13A3/A4, T13C9/C10, T13E5/E6 and T13G7/G8) scattered among 44 pairs of papillation mutants (Fig. 2A, cell patches with no mark). It was printed onto three different types of solid agar plates, LB, sporulation and milk, and we compared the cell patch morphology between papillation mutants and the wild type.

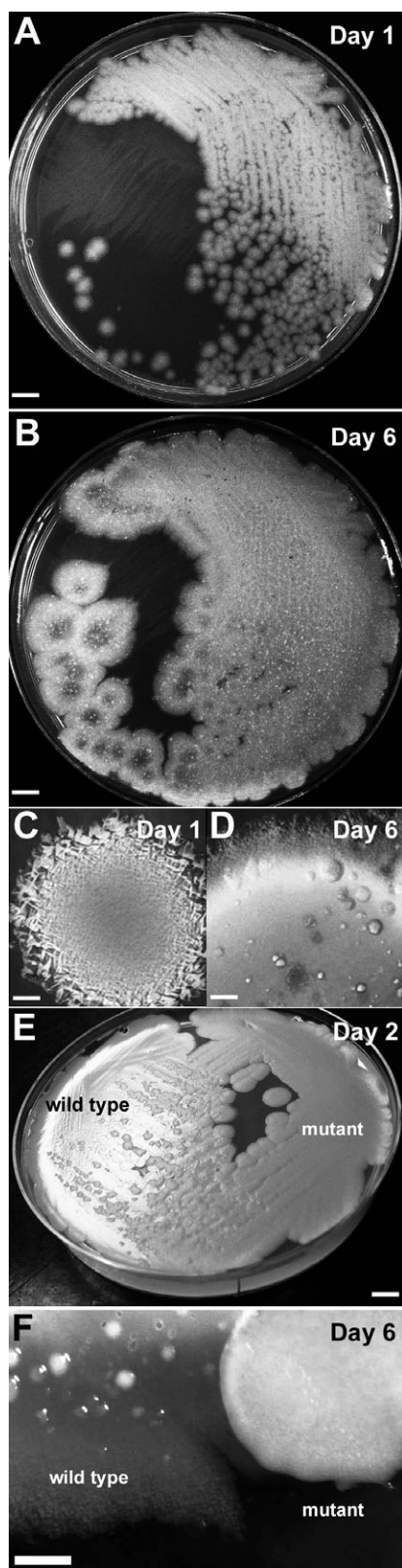


Fig. 1. Photographs of wild-type *B. anthracis* Sterne cells and papillation mutants grown on LB plates at 30°C. A. Wild-type colonies on day 1 (after 24 h at 30°C). Scale bar = 1 cm. B. Wild-type colonies on day 6. Papillae appear as white dots on the surface of parental colonies. Scale bar = 1 cm. C. A magnified image of a wild-type colony on day 1. Scale bar = 0.1 cm. D. A magnified image of a wild-type colony on day 6. Scale bar = 0.1 cm. E. Both a wild type and a papillation mutant were streaked on the same LB plate in a pattern where the colonies overlapped at the centre. Scale bar = 0.5 cm. F. A magnified image of a papillation mutant and a wild-type colony on day 6. While papillae appear on the surface of the wild-type colony, no visible papillae seen on the mutant colony. Scale bar = 0.1 cm.

On LB plates, after a 1 day of incubation at 30°C we observed similar appearances among individual cell patches (data not shown). After 2 days, the cell patches expanded to their full size and the majority still looked similar to each other except for some cell patches that started to display subtle differences in patch colour (Fig. 2A and B). After 6 days, while wild-type cells formed opaque cell patches (Fig. 2C, cell patches marked with grey brackets: T13C9/C10, T13E5/E6, and T13G7/G8), we observed at least two distinct patterns within the papillation mutants. One type formed an opaque patch with a halo at the centre (designated as group A; Fig. 2C, cell patches marked with black brackets). The other type formed a transparent patch occasionally with a thin/opaque rim (designated as group B; Fig. 2C, four pairs of colony patches marked with white brackets: T13D7/8, T13E3/E4, T13F9/F10 and T13G3/G4). The group B mutants showed subtle variations, which suggest that this group may contain more than one type of mutation. It is worth noting that while the cell patches of the wild-type control displayed papillation, almost all cell patches of the papillation mutants (233/243) displayed no visible papillae (data not shown). Failure to form solid opaque cell patches suggests that both groups A and B papillation mutants are defective in sporulation to various degrees on LB plates and we confirmed it by microscopic observations of several representatives (Fig. 2F): T13E5 (wild type), T13C3 (group A) and T13G3 (group B). While wild-type T13E5 contained mainly spores at both centre and the edge of its cell patch on the LB plate, T13C3 (group A) contained mainly rod-shaped cells at the centre and spores at the edge. However, T13G5 (group B) contained mainly rod-shaped cells at both centre and the edge.

On sporulation plates, wild-type cells formed white patches after a 3 day incubation at 30°C with very little change during the next few days (Fig. 2D, cell patches marked with grey brackets: T13C9/C10, T13E5/E6 and T13G7/G8). The group A mutants also formed white patches (Fig. 2D, colony patches marked with black

Fig. 2. Photographs of cell patches and cell morphology of a 96-well plate grown on different types of solid agar plates. Four pairs of wild-type controls, T13A3/A4, T13C9/C10, T13E5/E6 and T13G7/G8, are marked with grey brackets. Group A papillation mutants are marked with black brackets. Four pairs of group B mutants, T13D7/8, T13E3/E4, T13F9/F10 and T13G3/G4, are marked with white brackets. A. Grown on the LB plate on day 2 (48 h) at 30°C. The rectangle marks the area shown in B (see below). Only the wild-type control pairs are marked with grey brackets. Papillation mutants are not marked. B. A magnified image of a partial area of A. Only the wild-type control pairs are marked with grey brackets. Papillation mutants are not marked. C. The same area as in B on day 6 at 30°C. D. The same area as in B on the sporulation (SM) plate on day 6 at 30°C. E. The same area as in B on the milk plate after overnight incubation at 37°C. F. Cell morphology at the centre and the edge of cell patches observed from LB and SM plates on Day 6.

tained mainly spores, while T13G3 (group B) contained mainly rod-shaped cells (Fig. 2F).

We also examined the extracellular protease production of papillation mutants using milk plates (see the following sections). On the milk plates, wild-type cells formed a clear ring around cell patches indicating that they contain robust extracellular protease activities (Fig. 2E marked with grey brackets: T13C9/C10, T13E5/E6 and T13G7/G8). The group A mutants, however, displayed very little or no clear area (Fig. 2E marked with black brackets), suggesting that they have much reduced extracellular protease activity. The group B mutants displayed various levels of protease activities (Fig. 2E marked with white brackets: T13D7/8, T13E3/E4, T13F9/F10 and T13G3/G4), again suggesting that this group may contain more than one type of mutation.

In summary, 243 papillation mutants were assigned to group A (59) or group B (184) according to their phenotypes on the LB, sporulation and milk plates. Group A mutants display opaque cell patches with a halo at the centre on the LB plates. They are proficient in forming spores on the sporulation plates and they show very little extracellular protease activities. Group B mutants display semitransparent cell patches (with occasional thin rims) on the LB plates. They are deficient to various degrees in forming spores on the sporulation plates and they show varying amounts of extracellular protease activities on the milk plates.

Mutations in the nprR gene detected in the group A mutants

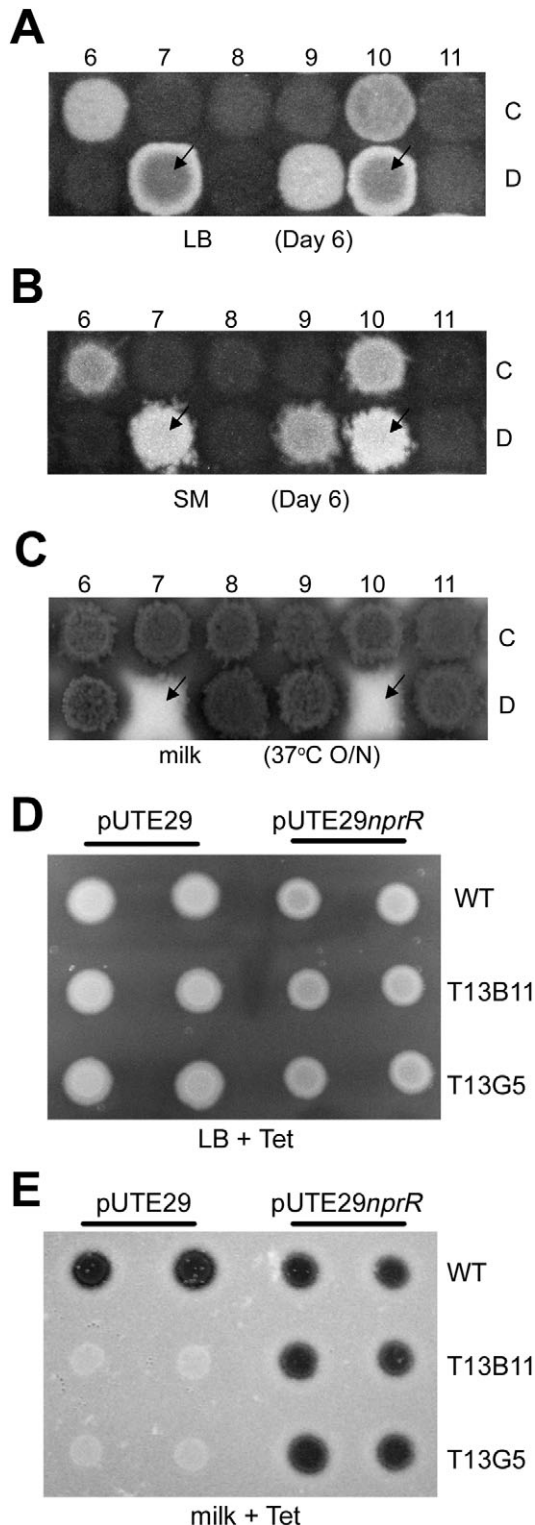
To identify genes that when mutated contribute to papillae formation, our strategy was to conduct a genome-wide transposon mutagenesis and search for transposon-insertion mutants that displayed phenotypes similar to the papillation mutants. The genes disrupted in those transposon-insertion mutants would serve as candidate genes, which would be further examined in the papillation mutants to determine whether any one of them was indeed mutated.

To conduct a genome-wide transposon mutagenesis, we developed a suicide vector pSV2 (see *Experimental procedures*) mediated transposon mutagenesis system to

deliver a *Himar1* minitransposon (McGillivray *et al.*, 2009) onto the *B. anthracis* chromosome. The transposon integration frequency of 4×10^{-6} can be achieved with $1-2 \times 10^9$ total surviving cells after electroporation to generate 4000–8000 independent transposon-insertion mutants in a single mutagenesis experiment. We searched for transposon-insertion mutants that displayed a good morphological resemblance to group A papillation mutants and the phenotypes of two such mutants, T17D7 and T17D10, are shown in Fig. 3. They formed opaque colony patches with a halo at the centre on the LB plates (Fig. 3A), were proficient in sporulation (Fig. 3B), and had much reduced extracellular protease activity (Fig. 3C). We were able to map the transposon-insertion sites in these mutants and discovered that gene BAS0566 encoding NprR, a neutral protease regulator that belongs to a Rap/NprR/PlcR/PrgX (or RNPP family) transcriptional regulator family (Declerck *et al.*, 2007; for a review, see Rocha-Estrada *et al.*, 2010), was independently disrupted (data not shown).

Is *nprR* indeed mutated in group A papillation mutants? We sequenced the *nprR* region in 59 group A mutants and in 58 cases detected mutations in the *nprR* gene. In one case the *nprR* region failed to be amplified by PCR using primers just outside of the *nprR*-coding region suggesting a large deletion may take place. In contrast, no mutations in *nprR* were seen in 15 mutants randomly chosen from group B. The mutations identified among the group A mutants can be classified into 42 different types ranging from single point mutations (13/42) to insertions (8/42) and deletions of various lengths (21/42, Table 1), which strongly indicates that the mutations lead to the loss of the NprR function. It is worth noting that three tandem duplications take place between 5 to 6 bp short homologous DNA sequences and 13 large deletions (≥ 5 bp) occur between 4 to 12 bp short homologous DNA sequences (Table 1). Similar DNA duplication/deletion patterns have been observed in *E. coli* (e.g. Farabaugh *et al.*, 1978; Miller and Albertini, 1983; Whoriskey *et al.*, 1987).

Can a wild-type *nprR* gene complement group A mutations? We introduced the wild-type *nprR* gene back to group A mutants and studied the extracellular protease production using pUTE29*nprR* – a shuttle plasmid pUTE29 (Koehler *et al.*, 1994) containing a wild-type



nprR coding region (pUTE29*nprR*, see *Experimental procedures*). Two mutants were chosen, T13B11 (Table 1, No. 39) and T13G5 (Table 1, No. 19). Each represents an *nprR* mutation in the categories of deletion or insertion respectively. Our results show that while the strains con-

Fig. 3. A–C. Photographs showing two transposon-insertion mutants T17D7 and T17D10 (marked with black arrows), which display similar phenotypes as the group A papillation mutants. D–E. photographs of cells harbouring pUTE29 or pUTE29*nprR* on LB and milk plates.

A. On the LB plate.

B. On the sporulation (SM) plate.

C. On the milk plate.

D. LB plate containing 5 mg l⁻¹ tetracycline.

E. Milk plate containing 5 mg l⁻¹ tetracycline.

taining either pUTE29 or pUTE29*nprR* grew on both LB and milk plates, only the papillation mutants that contain pUTE29*nprR* (as well as the wild type) were able to form a clear area on the milk plates indicating that the wild-type *nprR* gene indeed rescued the extracellular protease production of these papillation mutants (Fig. 3D and E).

Mutators with elevated levels of papillation

We observed that occasional *B. anthracis* transposon-insertion mutants displayed elevated levels of papillation, indicative of a mutator phenotype (see *Introduction*). Initial mapping of the transposon-insertion sites in two of such mutants, SV17D9 and T6F8 (Fig. 4A), revealed that they disrupt DNA mismatch repair genes, *mutS* and *mutL* respectively (Table 2, No. 1 and 2). Therefore, we decided to use papillation as a tool to conduct a genome-wide search for mutators that would display elevated levels of papillation. After screening ~10 000 transposon-insertion mutants, we found candidates that displayed various elevated levels of papillation. The transposon insertion sites of the candidates were mapped and those with verified mutator phenotypes in the subsequent study are listed in Table 2. Among eight additional strong to very strong papillation mutants one insert was in the *mutS* gene (Table 2, No. 3) and seven in a small region on the *B. anthracis* chromosome, where three genes, *yycH*, *yycI* and *yycJ*, are located (Table 2, No. 4–10). The papillation patterns of each representative *yycH*, *yycI* and *yycJ* mutant are shown in Fig. 4B. Two moderate to strong papillation mutants were mapped in *mutY* and *recJ* respectively (Table 2, No. 11–12).

We focused on three genes, *yycH*, *yycI* and *yycJ*, as disruption of these genes lead to a strong papillation phenotype. *YycH*, *yycI* and *yycJ* belong to the same operon that includes three other genes: *yycF*, *yycG* and a *degQ* homologue gene (Fig. 4C). *YycF* and *yycG* encode a two-component system (YycG/YycF or Walk/WalR) that is specific to low G + C Gram-positive bacteria (Szurmant *et al.*, 2007a; 2008; Dubrac *et al.*, 2008; Fukushima *et al.*, 2008). WalkR has been reported to be essential for cell viability in several pathogens and critical for maintaining cell wall homeostasis (Dubrac *et al.*, 2008). While the function of YycJ is uncertain, YycH and YycI have been

Table 1. Mutations in *nprR* (BAS0566).

| No. | Type of change | BAS0566 | Occurrence | Sequence ^a |
|-----------------|--------------------|------------------------------|------------|--|
| Group A mutants | | | | |
| 1 | Base substitution | A → G, promoter region | 1 | |
| 2 | Base substitution | 31, C → T | 1 | CAA (gln) → TAA (ochre) |
| 3 | Base substitution | 112, A → G | 2 | AAA (lys) → GAA (glu) |
| 4 | Base substitution | 133, G → T | 1 | GAA (glu) → TAA (ochre) |
| 5 | Base substitution | 140, C → T | 1 | TCA (ser) → TTA (leu) |
| 6 | Base substitution | 160, C → T | 1 | CTC (leu) → TTC (phe) |
| 7 | Base substitution | 772, G → T | 1 | GAG (glu) → TAG (amber) |
| 8 | Base substitution | 862, C → T | 1 | CAA (gln) → TAA (ochre) |
| 9 | Base substitution | 904, C → T | 1 | CAA (gln) → TAA (ochre) |
| 10 | Base substitution | 914, T → G | 1 | TTA (leu) → TGA (opal) |
| 11 | Base substitution | 980, C → A | 4 | GCA (ala) → GAA (glu) |
| 12 | Base substitution | 1055, T → G | 1 | TTA (leu) → TGA (opal) |
| 13 | Base substitution | 1178, T → C | 1 | CTA (leu) → CCA (pro) |
| 14 | Insertion | 17, extra 1 bp | 1 | 6A → 7A |
| 15 | Insertion | 461, extra 1 bp | 1 | 1T → 2T |
| 16 | Insertion | 580, extra 1 bp | 1 | 2A → 3A |
| 17 | Insertion | 844, extra 1 bp | 2 | 6A → 7A |
| 18 | Insertion | 867, extra 1 bp | 2 | 7A → 8A |
| 19 | Tandem duplication | 121–135, 15 bp | 1 | <u>GTAAATCGAA</u> AATGGAAAGATCGAA AATGGAAAGATCGAA GCATC |
| 20 | Tandem duplication | 319–325, 7 bp | 1 | AGCATGTTTTG <u>GATTTTG</u> <u>GATTTTG</u> AAATTA |
| 21 | Tandem duplication | 479–558, 80 bp | 1 | <u>TAGAGGGTTAT</u> TGTGC . . . <u>CAAGGTTAT</u> TGTGC . . . <u>CAAGGTTAT</u> CATGA |
| 22 | Deletion | 56, Δ1 bp | 1 | 6A → 5A |
| 23 | Deletion | 377, Δ1 bp | 1 | 3G → 2G |
| 24 | Deletion | 768, Δ2 bp | 1 | 3GA → 2GA |
| 25 | Deletion | 844, Δ1 bp | 1 | 6A → 5A |
| 26 | Deletion | 850, Δ1 bp | 2 | 2G → 1G |
| 27 | Deletion | 867, Δ1 bp | 6 | 7A → 6A |
| 28 | Deletion | 1074, Δ1 bp | 1 | 4T → 3T |
| 29 | Deletion | 1045, Δ1 bp | 1 | GAGAGGTTAATGCAAAATTA TACTTGCTTTAATGCTTAGATATAAAT |
| 30 | Large deletion | 117, Δ7 bp | 1 | ATACTTAAGT AAAAAT <u>CGAAAAAT</u> GGAAAAGA |
| 31 | Large deletion | 122, Δ7 bp | 2 | AAGTAAATCGAAA <u>ATGGAAA</u> GATCGAA |
| 32 | Large deletion | 141, Δ697 bp | 1 | AAGATCGAAGCATC <u>AGAAGAG</u> . . . <u>TATGGGAAGCATC</u> TATTATAA |
| 33 | Large deletion | 215, Δ18 bp | 1 | ATGTAGAAGAGGATG <u>TGAAGGGGAAGCTGGATG</u> AATGGTTA |
| 34 | Large deletion | 213, Δ11 bp | 1 | GATGTAGAAGAGGA <u>TGTGAAGGGGA</u> AGCTGGA |
| 35 | Large deletion | 319, Δ7 bp | 1 | ATGAAGCATGTTTTG <u>GATTTTG</u> AAATTATA |
| 36 | Large deletion | 341, Δ582 bp | 1 | GAAATTATAAATTATT <u>ATAAACTG</u> . . . <u>GATTAAATTATT</u> TAGATACA |
| 37 | Large deletion | 401, Δ20 bp | 1 | CTACACT GAAGAAG <u>AATTAGATAGATTGAAGAAG</u> GTATATAA |
| 38 | Large deletion | 784, Δ55 bp | 1 | AGAGAGTCCGCATCT <u>TTTGCTGAT</u> . . . <u>GGGAA GCATCT</u> ATTATAAA |
| 39 | Large deletion | 797, Δ204 bp | 1 | CTTTTGCTGATAAGG <u>ATGTACT</u> . . . <u>ATTAATTGATAAGG</u> GAATTG |
| 40 | Large deletion | 887, Δ42 bp | 4 | AAATATTATTAGATA <u>GTCTAC</u> . . . <u>TTAAATTATTAGATA</u> CAATATA |
| 41 | Large deletion | 1148, Δ5 bp | 1 | AATCTGCGG AAATA <u>AAATA</u> GAATTAAA |
| 42 | Large deletion | 1269, Δ66 bp | 1 | TGATAAGG GAATA <u>AAAATGA</u> . . . <u>TTGCTGGAGGAATA</u> CATCAGTA |
| Undetermined | | | 1 | |
| Total | | | 59 | |
| Group B mutants | | | | |
| Total | | BAS0566 | Occurrence | |
| 15 | | no error | 15 | |

a. Tandem duplication and deletion sequences are underlined. Short homologous sequences are in bold.

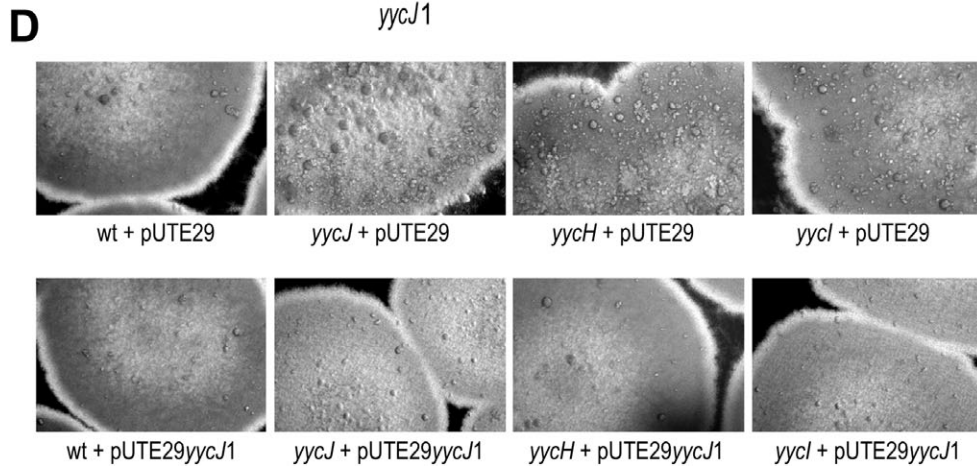
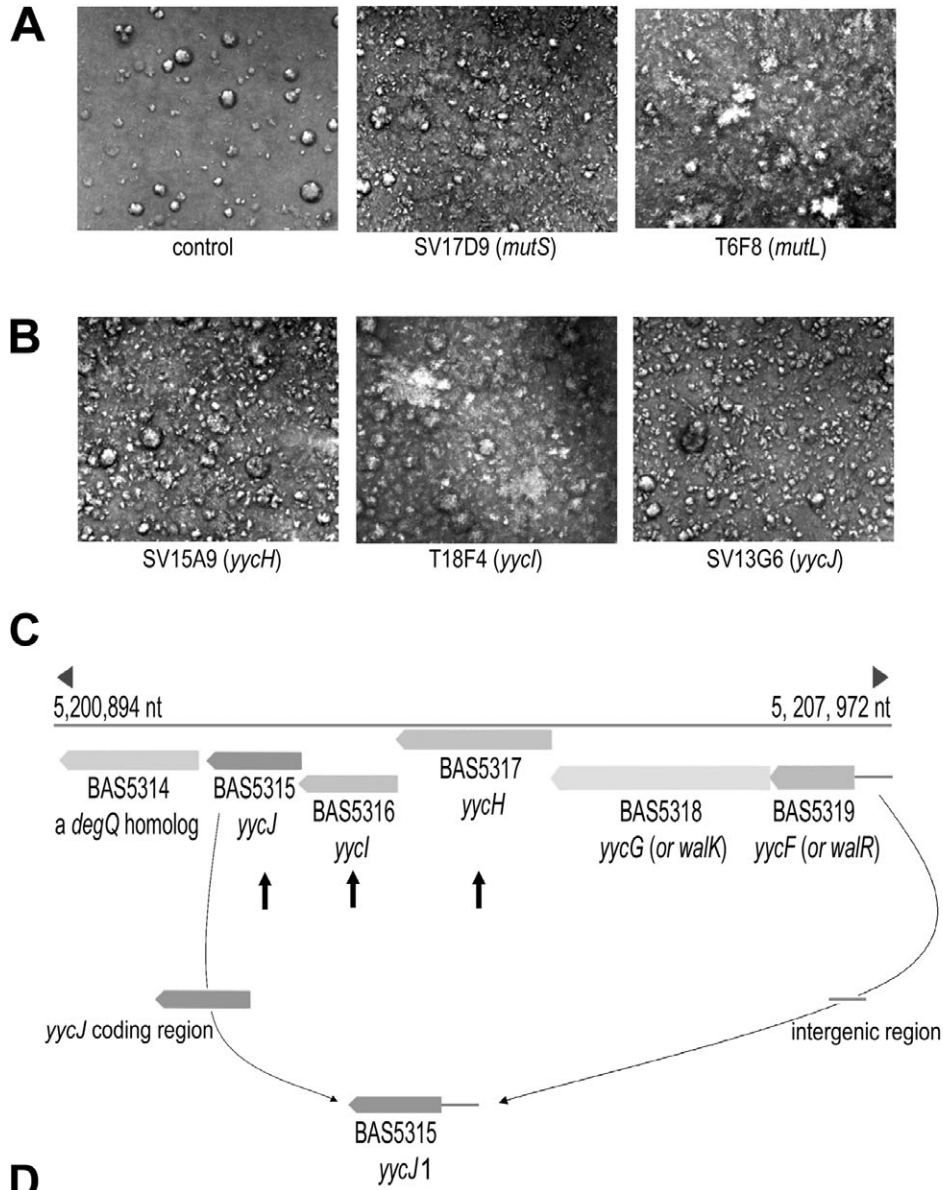


Fig. 4. Mutants with elevated levels of papillation.

A. Photographs of the colony patches of two transposon-insertion mutants, SV17D9 (*mutS*) and T6F8 (*mutL*), and the wild type (control) after 6 days at 30°C on an LB plate. Papillae appear as bright dots on the grey surface of colony patches.

B. Photographs of the colony patches of three transposon-insertion mutants, SV15A9 (*yycH*), T18F4 (*yycI*) and SV13G6 (*yycJ*), which display elevated levels of papillation after 6 days at 30°C on an LB plate. Papillae appear as bright dots on the grey surface of colony patches.

C. A schematic diagram of the *WalkR* operon in *B. anthracis*. Three genes, *yycH*, *yycI* and *yycJ*, are marked with black arrows. The *yycJ1* construct contains the intergenic region located upstream of the *walkR* operon and the *yycJ* coding region.

D. Photographs of the colonies containing the vector pUTE29 alone or the vector with the *yycJ1* construct, pUTE29*yycJ1*, after 6 days at 30°C on LB plates. Papillae appear as dots on the grey surface of the colonies.

shown to play a role in negatively controlling the *WalkR* regulon (Szurmant *et al.*, 2007b). Because the *yycJ* gene is located downstream of *yycH* and *yycI*, it is possible that the transposon insertions in *yycH* and *yycI* cause a polar effect on the *yycJ* gene. To test this hypothesis, we conducted a complementation experiment using pUTE29*yycJ1* containing a wild-type *yycJ* coding region fused with the intergenic region located upstream of the *walkR* operon (*yycJ1*, Fig. 4C). A pUTE29 vector alone was also included in the experiment as a negative control. Our results show that pUTE29*yycJ1* not only lowered the level of papillation in the *yycJ* mutant, but also lowered the levels of papillation in both *yycH* and *yycI* mutants (Fig. 4D). Therefore, our results show that the lack of the functional *yycJ* is the cause of the elevated levels of papillation seen in the *yycJ* mutants as well as in *yycH* and *yycI*. It also eliminated the possibility of any polar effect on the 6th gene in the operon (BAS5314) being the cause of the mutator phenotype.

We used a representative *yycJ* mutant SV13G6 and measured its mutation frequency in the *rpoB* gene that leads to the Rif^r phenotype in the presence or absence of the wild-type *yycJ* gene (Table 3). Our results show that the Rif^r frequency of this *yycJ* mutant is 402×10^{-9} , which is about 120-fold above the wild-type level, and comparable with that of the mismatch deficient strain *mutS* (Zeibell *et al.*, 2007), indicating that the *yycJ* mutant is indeed a very strong mutator. In the presence of the

wild-type *yycJ* gene, however, the Rif^r frequency of SV13G6 was lowered to 1.5×10^{-9} indicating complete complementation. We further studied the mutational specificities of the *yycJ* mutant using the *rpoB*/Rif^r mutational analysis system (Vogler *et al.*, 2002; Zeibell *et al.*, 2007) and the results show that the *yycJ* mutant has similar mutational specificity as mismatch repair deficient mutants, namely it favours transition base substitutions at the two sites (1403 and 1442, data not shown) identified previously (Zeibell *et al.*, 2007) and no hits at the site 1441 (data not shown), one of the prominent sites in the wild type (Zeibell *et al.*, 2007).

We also measured the Rif^r frequency of T18E7, the *recJ* mutant (Table 3). It displayed the Rif^r frequency of 3.1×10^{-9} , indicating that in *recJ* the base substitution rate is quite similar to that of the wild type. This suggests that the increased level of papillation in the *recJ* mutant may be due to mutations other than base substitutions (see the following section).

nprR/papillation mutational analysis system and *yycJ* mutational spectrum

While the *rpoB*/Rif^r system only detects limited sites of base substitutions in the *rpoB* gene, the mutational spectrum of the *nprR* gene from the wild-type group A papillation mutants reveals frameshift mutations, tandem duplications and large deletions in addition to many avail-

Table 2. Transposon insertion sites in mutants that display elevated levels of papillation.

| No. | Location ^a | Tn-insertion site (bp) | % ^b | Gene | Transcription direction | Function |
|-----|-----------------------|------------------------|----------------|---------|-------------------------|--|
| 1 | SV17D9 | 3579425 | 40 | BAS3618 | ← | MutS, DNA mismatch repair protein |
| 2 | T6F8 | 3577328 | 25 | BAS3617 | ← | MutL, DNA mismatch repair protein |
| 3 | T18B1 | 3580350 | 5 | BAS3618 | ← | MutS, DNA mismatch repair protein |
| 4 | SV15A9 | 5204317 | 59 | BAS5317 | ← | YycH protein |
| 5 | SV24F1 | 5204333 | 58 | BAS5317 | ← | YycH protein |
| 6 | T18E9 | 5204683 | 31 | BAS5317 | ← | YycH protein |
| 7 | T18E12 | 5204702 | 29 | BAS5317 | ← | YycH protein |
| 8 | T18F4 | 5203102 | 82 | BAS5316 | ← | YycI protein |
| 9 | SV13G6 | 5202503 | 59 | BAS5315 | ← | YycJ, metallo-beta-lactamase family protein |
| 10 | T18E7 | 5202921 | 6 | BAS5315 | ← | YycJ, metallo-beta-lactamase family protein |
| 11 | T18E5 | 4216477 | 48 | BAS4304 | ← | RecJ, single-stranded DNA-specific exonuclease |
| 12 | T18F2 | 515949 | 84 | BAS0491 | → | MutY, A/G-specific adenine glycosylase |

a. On 96-well plates.

b. (Length between start codon and Tn-insertion site)/(Length of the ORF) × 100.

Table 3. *B. anthracis* *rpoB* mutation frequencies.

| Genotype | f × 10 ⁹ |
|---|---------------------------|
| Wild type | 3.2 (0–12.8) ^a |
| SV13G6 (<i>yycJ</i>) | 402 (223–522) |
| SV13G6 (<i>yycJ</i>) + pUTE29 | 469 (420–661) |
| SV13G6 (<i>yycJ</i>) + pUTE29 <i>yycJ1</i> ^b | 1.5 (0–1.5) |
| T18E5 (<i>recJ</i>) | 3.1 (0–7.9) |

a. Values in parentheses are 95% confidence limits (Dixon and Massey, 1969).

b. This construct contains a 6His-tag at the N-terminus of the *YycJ* protein.

able sites for the base substitution mutations (Table 1). Therefore, it would be advantageous to use the *nprR* papillation system as a mutational analysis system as it would provide additional insights into the mechanisms of action of mutators.

To use the *nprR*/papillation system for the mutational spectrum of the *yycJ* mutant (SV13G6), we first isolated the group A papillation mutants from the *yycJ* background and then examined the mutation spectra of the *nprR* gene. As a calibration for this new system, we also included two known mutators in the study, *mutS* (SV17D9, Table 2) and *mutY* (T18F2, Table 2). We found that the mutation spectra derived from the *yycJ* and *mutS* background were quite similar. The majority consisted of small insertions/deletions in runs of 6As and 7As (40/58 from the *yycJ* mutant, 40/70 from the *mutS* mutant, versus 13/58 from the wild type). Very few tandem duplication/large deletions were detected in both *yycJ* and *mutS* mutants, in contrast to the wild type (2/58 from the *yycJ* mutant, 1/70 from the *mutS* mutant and 20/58 from the wild type). The base substitution mutations in the *yycJ* background were mainly A : T → G : C or G : C → A : T transitions, which is consistent with the *mutS* mutator phenotype in *B. anthracis* (Table 4; Zeibell *et al.*, 2007). While G : C → T : A mutations were also prominent in the wild type, they were not detected in either the *yycJ* or *mutS* mutant (Table 4). As expected, 10/12 mutations in the *mutY* background were G : C → T : A transversions, compared with only 6/58 found in the wild type.

recJ mutational spectrum

We analysed the mutational spectrum of the transposon-insertion mutant *recJ* (T18E5) in the *nprR* gene that lead to group A papillation mutants (designated as *recJ* in Table 4). We also constructed and analysed an independent *recJ* mutant by a suicide vector mediated gene disruption (designated as *recJ'* in Table 4, see *Experimental procedures*). Both mutants show similar mutational specificities, namely, the vast majority of mutations were tandem duplications (49/63 and 27/37 detected in the *recJ*

and *recJ'* mutant, respectively; Table 4) in contrast to the wild-type spectrum, where only three cases were seen (3/58). The two most frequently detected tandem duplications occur in one case in a region that already contains a 7 bp tandem duplication 'AAATTAT' (Table 5, No. 1), and in the other in a region that contains an 8 bp repeat of 'TTAAATTA' separated by 35 bp DNA (Table 5, No. 2).

Discussion

Papillation mutants and extension of vegetative growth

Traditional papillation takes place in an environment where wild-type cells undergo growth arrest due to the lack of nutrients. Papillation mutants are actively growing cells proficient in utilizing secondary nutrients that normal wild-type cells are unable to use. Owing to a complicated life cycle, papillation in *B. anthracis* has its unique features. It takes place when wild-type cells undergo sporulation. *B. anthracis* papillation mutants are a group of heterogenous mutants that are capable of maintaining active cell division for an extended period of time. They appear as morphological variants as they show growth advantage over the wild-type cells during this extended growth period, and can be readily distinguished from the wild type as a result of their unique characteristic light reflection features. Because the transition between vegetative growth and sporulation is governed by multiple environmental signals such as nutritional, cell density and cell cycle signals (for review, see Kroos, 2007), the genes that are responsible for papillae formation are likely to be involved in the early decision-making process of sporulation. Therefore, identification of these genes can potentially uncover multiple environmental signalling pathways that ultimately channel to the decision-making regulator.

In this study we identified one such gene, *nprR*, which leads to the group A papillation mutants when mutated. The *nprR* gene encodes a transcriptional regulator NprR, which shares a structural similarity to PlcR, the major virulence regulator of the *Bacillus cereus* group (Declerck *et al.*, 2007). PlcR is widely distributed in the *B. cereus* group and upregulates various virulence factors through its quorum sensing, i.e. the regulation of gene expression according to population densities (Declerck *et al.*, 2007). However, the *plcR* gene in *B. anthracis* is inactivated because of the presence of a nonsense mutation in its coding region (Kolstø *et al.*, 2009). From structural and phylogenetic analysis it has been postulated that Npr transcriptional regulators are quorum sensors (Declerck *et al.*, 2007). This study provides for the first time the biological evidence of the NprR action and papillation in *B. anthracis*. We speculate that NprR is one of the early sensors that ultimately affect the decision-making appa-

Table 4. Distribution of mutations in *nprR* from group A papillation mutants.

| Type of change | Detected sites ^a | WT | <i>yycJ</i> | <i>mutS</i> | <i>mutY</i> | <i>recJ</i> | <i>recJ</i> |
|--------------------------|-----------------------------|-------|-------------|-------------|-------------|-------------|-------------|
| AT → GC | 7 | 4 | 7 | 3 | 0 | 0 | 1 |
| GC → AT | 19 | 5 | 3 | 10 | 1 | 1 | 1 |
| AT → TA | 2 | 0 | 1 | 0 | 0 | 0 | 1 |
| GC → TA | 14 | 6 | 0 | 0 | 10 | 1 | 1 |
| AT → CG | 3 | 2 | 0 | 1 | 0 | 0 | 0 |
| Base substitutions/total | | 17/58 | 11/58 | 14/70 | 11/12 | 2/63 | 4/37 |
| 1A → 2A | 1 | 0 | 0 | 1 | 0 | 0 | 0 |
| 1T → 2T | 1 | 1 | 0 | 0 | 0 | 0 | 0 |
| 2A → 3A | 1 | 1 | 0 | 0 | 0 | 0 | 0 |
| 4A → 5A | 1 | 0 | 0 | 0 | 0 | 1 | 0 |
| 5A → 6A | 3 | 0 | 1 | 4 | 0 | 0 | 0 |
| 5T → 6T | 2 | 0 | 1 | 3 | 0 | 0 | 0 |
| 6A → 7A | 3 | 3 | 16 | 18 | 0 | 0 | 0 |
| 7A → 8A | 1 | 2 | 6 | 4 | 0 | 0 | 1 |
| 4G → 5G | 2 | 0 | 0 | 4 | 0 | 2 | 0 |
| 3AT → 4AT | 1 | 0 | 0 | 1 | 0 | 0 | 1 |
| Small insertions/total | | 7/58 | 24/58 | 35/70 | 0/12 | 3/63 | 2/37 |
| Tandem dup. | 32 | 3 | 1 | 0 | 0 | 49 | 27 |
| Tandem dup./total | | 3/58 | 1/58 | 0/70 | 0/12 | 49/63 | 27/37 |
| Δ1A | 1 | 0 | 0 | 1 | 0 | 0 | 0 |
| Δ1T | 1 | 1 | 0 | 0 | 0 | 0 | 0 |
| 4T → 3T | 1 | 1 | 0 | 0 | 0 | 0 | 0 |
| 5T → 4T | 1 | 0 | 1 | 0 | 0 | 0 | 0 |
| 5A → 4A | 1 | 0 | 0 | 0 | 0 | 2 | 0 |
| 6A → 5A | 3 | 2 | 8 | 7 | 0 | 0 | 0 |
| 7A → 6A | 1 | 6 | 10 | 11 | 0 | 0 | 1 |
| 2G → 1G | 1 | 2 | 0 | 1 | 0 | 0 | 0 |
| 3G → 2G | 2 | 1 | 1 | 0 | 0 | 1 | 0 |
| 4G → 3G | 1 | 0 | 1 | 0 | 0 | 0 | 0 |
| 3GA → 2GA | 1 | 1 | 0 | 0 | 0 | 1 | 0 |
| Small deletions/total | | 14/58 | 21/58 | 20/70 | 0/12 | 4/63 | 1/37 |
| Δ5 bp | 1 | 1 | 0 | 0 | 0 | 0 | 0 |
| Δ7 bp | 4 | 4 | 1 | 0 | 0 | 0 | 0 |
| Δ10 bp | 1 | 0 | 0 | 1 | 0 | 0 | 0 |
| Δ11 bp | 1 | 1 | 0 | 0 | 0 | 0 | 0 |
| Δ18 bp | 1 | 1 | 0 | 0 | 0 | 0 | 0 |
| Δ20 bp | 1 | 1 | 0 | 0 | 0 | 1 | 0 |
| Δ23 bp | 1 | 0 | 0 | 0 | 1 | 0 | 0 |
| Δ42 bp | 1 | 4 | 0 | 0 | 0 | 0 | 0 |
| Δ43 bp | 1 | 0 | 0 | 0 | 0 | 0 | 1 |
| Δ55 bp | 1 | 1 | 0 | 0 | 0 | 1 | 0 |
| Δ66 bp | 1 | 1 | 0 | 0 | 0 | 0 | 0 |
| Δ87 bp | 1 | 0 | 0 | 0 | 0 | 1 | 1 |
| Δ204 bp | 1 | 1 | 0 | 0 | 0 | 0 | 0 |
| Δ276 bp | 1 | 0 | 0 | 0 | 0 | 0 | 1 |
| Δ465 bp | 1 | 0 | 0 | 0 | 0 | 1 | 0 |
| Δ483 bp | 1 | 0 | 0 | 0 | 0 | 1 | 0 |
| Δ582 bp | 1 | 1 | 0 | 0 | 0 | 0 | 0 |
| Δ697 bp | 1 | 1 | 0 | 0 | 0 | 0 | 0 |
| Large deletions/total | | 17/58 | 1/58 | 1/70 | 1/12 | 5/63 | 3/37 |
| Not determined | | 1 | 0 | 0 | 0 | 4 | 0 |
| Total | | 59 | 58 | 70 | 12 | 67 | 37 |

a. Unique sites detected.

ratus to initiate sporulation. NprR mutants undergo sporulation just as well as the wild type on sporulation medium; however, they fail to initiate sporulation when grown on LB medium (with the exception of cells at the edge of the cell patch). Additional experiments are needed to determine the molecular mechanisms of the NprR action and its impact on virulence. It is worth noting that putative mature penta-peptides have been proposed for both *Bacillus thu-*

ringiensis NprR and *Bacillus stearothermophilus* NprA (Pottathil and Lazazzera, 2003).

It appears that more than half of the *nprR* missense mutation sites identified so far (11/18) are clustered within the first 60 amino acid residuals of the NprR protein (Fig. 5). It has been proposed that this region corresponds to the N-terminal helix–turn–helix DNA binding domain in the Rap/NprR/PlcR/PrgX transcriptional regulator family

Table 5. Tandem duplications detected in the *recJ* mutants.

| No. | BAS0566 | Occurrence ^a | Sequence ^b |
|-------|------------------|-------------------------|--|
| 1 | 333–339, 7 bp | 17 | ATTTTGAATAT |
| 2 | 921–963, 43 bp | 12 | <u>TTTAGAT ... ATGCATTAATAA</u> TTAGAT ... ATGCATTAATAA |
| 3 | 237–244, 8 bp | 4 | GTTAAATG |
| 4 | 588–644, 57 bp | 4 | GCTGGATGAATG |
| 5 | 1011–1060, 50 bp | 4 | ATTATAATATAGC |
| 6 | 222–237, 16 bp | 3 | GGGAATGATGC |
| 7 | 401–420, 20 bp | 3 | GGATGTGAAGGG |
| 8 | 336–345, 10 bp | 2 | CAC TTGAAGAAG |
| 9 | 338–347, 10 bp | 2 | TTGAAATTAATAA |
| 10 | 384–426, 43 bp | 2 | GAAATTAATAA TT |
| 11 | 425–435, 11 bp | 2 | GAAAAGGGATAT |
| 12 | 463–500, 38 bp | 2 | TGAAGAAGGTAT |
| 13 | 616–630, 15 bp | 2 | GTTATTATATG |
| 14 | 968–999, 32 bp | 2 | TTTAGATATTAT |
| 15 | 87–220, 134 bp | 1 | TTAAATTAGAG |
| 16 | 133–140, 8 bp | 1 | ATTATGTCAGGG |
| 17 | 213–223, 11 bp | 1 | AATGGAAGATC |
| 18 | 225–304, 80 bp | 1 | TGTAGAAGAGGA |
| 19 | 230–237, 8 bp | 1 | AGGGGAAGCTGG |
| 20 | 326–385, 60 bp | 1 | GTTTTGGATTTG |
| 21 | 418–504, 87 bp | 1 | AGATAGATTGAAG |
| 22 | 422–508, 87 bp | 1 | AGATAGATTGAAGAAGG |
| 23 | 509–554, 46 bp | 1 | ATGGAAGGAGG |
| 24 | 599–670, 72 bp | 1 | CGCTTGATATA |
| 25 | 736–781, 46 bp | 1 | AAAGGTCAAGTAT |
| 26 | 809–821, 13 bp | 1 | GATGACTTTTAG |
| 27 | 821–900, 80 bp | 1 | GCTATTACTTTAA |
| 28 | 1038–1060, 23 bp | 1 | GAGGTTAATGC |
| 29 | 1136–1172, 37 bp | 1 | CGTTGTATAAAT |
| Total | | 76 | |

a. Tandem duplications detected in *recJ* and *recJ* mutants.

b. Tandem duplication sequences are underlined. Short homologous sequences are in bold.

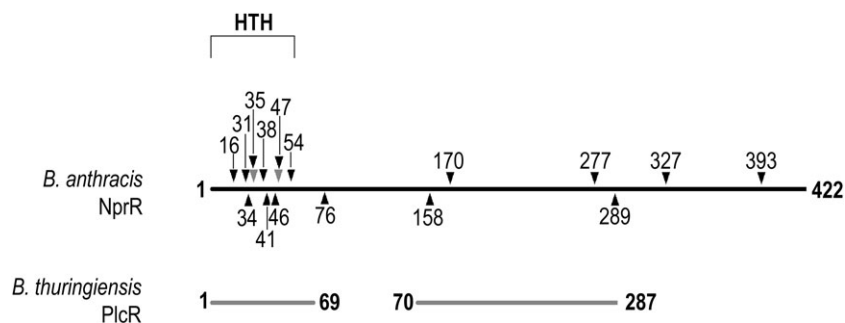


Fig. 5. A schematic diagram of the *nprR* missense mutations. The protein sequences are drawn as horizontal lines. The independent missense mutations are marked as arrows. Different missense mutations took place within the same codon can be distinguished as black and grey arrows pointed to the same location on the protein sequence. The alignment between NprR and PlcR is according to Declerck *et al.*, 2007 using *B. anthracis* NprR. NCBI (<http://www.ncbi.nlm.nih.gov/protein>) accession numbers are as follows: *B. anthracis* NprR, YP_026843 and *B. thuringiensis* PlcR, ZP_00739149.

(Pottathil and Lazazzera, 2003; Declerck *et al.*, 2007). Therefore, we speculate that these single missense mutations in the HTH domain can severely abolish the DNA binding ability of the NprR protein and thus result in much reduced NprR activity.

Papillation as a tool for finding mutators

In this study we demonstrate that papillation in *B. anthracis* is a powerful tool for detecting mutators, similar to studies that have been carried out in *E. coli*. In addition to finding previously identified mutators such as *mutL*, *mutS* and *mutY* (Table 2), we identified two additional mutators. One, *recJ*, has not been found to be a spontaneous mutator in the absence of other mutations. Interestingly, it has a unique specificity, stimulating only tandem duplications, a majority of which is at short sequence repeats, often but not always separated by a stretch of bp (see Table 5). That one finds duplications but not deletions is striking. It appears that the lengths of the stretch are usually less than 100 bp (28/29 independent cases, Table 5) and the majority of the duplications leads to frameshifts (23/29 independent cases, Table 5). Analysing the *nprR* DNA sequence also supports the above hypothesis. The *nprR* gene contains a total of 60 independent short sequence repeats ranging from 8 to 12 bp (perfect match, data not shown); however, in only 6 cases (6/60) are the short sequence repeats separated by less than 100 bp and 4 out of these 6 cases generate frameshifts. We have detected 5 out of these 6 cases, the sixth case being a duplication that does not generate a frameshift. RecJ has been previously studied extensively in both *E. coli* (e.g. Han *et al.*, 2006; Dutra *et al.*, 2007), and other organisms, such as *Haemophilus influenzae* (Kumar *et al.*, 2008). RecJ is a single-stranded exonuclease (Han *et al.*, 2006, and references therein) that is a redundant function for mismatch repair (Viswanathan *et al.*, 2001), and also for the stabilization of tandem

repeats in *E. coli* (Feschenko *et al.*, 2003). We also identified a new spontaneous mutator *yycJ*. The *yycJ* mutant displays a much higher level of papillation than wild type and its mutational spectrum is similar to that of the mismatch repair-deficient mutant *mutS* (Fig. 4B and Table 3). So far, the precise function of the YycJ protein is not yet known. It has been reported that *B. subtilis* cells carrying an in-frame deletion of *yycJ* results in altered colony morphology and increased frequency in production of sporulation-deficient colonies (Szurmant *et al.*, 2007b). We can explain increased frequency in production of sporulation-deficient colonies by its genomic instability as a result of the deletion of the *yycJ* gene. It has also been reported that a YycJ homologue is conditionally essential for expression of the *yycF* response regulator (Ng *et al.*, 2003) and in another case it modulates *gtfB/C* expression, biofilm formation, genetic competence and oxidative stress tolerance (Senadheera *et al.*, 2007). In low G + C Gram-positive bacteria, the *yycJ* gene is located in the *walkR* operon crucial for cell wall metabolism (Dubrac *et al.*, 2008). It has the metallo-beta lactamase fold that is also shared by several DNA double-stranded break repair nucleases (e.g. Artemis) (Dominski, 2007). Experiments elucidating the possible role of YycJ in DNA mismatch repair are in progress.

nprR/papillation mutational analysis system

The *nprR*/papillation system is a valuable new mutational analysis system. In contrast to the *rpoB*/Rif^r system in *B. anthracis* (Vogler *et al.*, 2002; Zeibell *et al.*, 2007), this new system allows detection of any mutation that disrupts NprR function, including frameshift mutations, tandem duplications, large deletions and base substitutions. We have used this system to demonstrate that the specificity of spontaneous mutations in *nprR* in different mutator backgrounds was different in each case, indicating that the mutations detected in this system are not caused by a

Table 6. Predicted number of base substitution sites in the *nprR* coding region.

| | AT → GC | GC → AT | GC → TA | AT → TA | AT → CG | GC → CG |
|----------------------|---------|---------|---------|---------|---------|---------|
| TAA + TAG predicted | 0 | 23 | 49 | 113 | 31 | 5 |
| Non-TAA/TAG detected | 6 | 7 | 2 | 2 | 3 | 0 |
| Total | 6 | 30 | 51 | 115 | 34 | 5 |

single mechanism, such as adaptive mutagenesis (see reviews by Foster, 2007 for *E. coli*, and Robleto *et al.*, 2007, for *B. subtilis*). The 45 independent base substitution mutational sites detected so far in the *nprR*-coding region already greatly exceed the sites in the *B. anthracis rpoB/Rif* system. How many potential base substitution sites exist in the *nprR* gene? NprR has 422 amino acids in length. More than half of the detected base substitutions result in amber UAG and ochre UAA (25/45) suggesting that a complete knockout of NprR activity is necessary in order to generate the mutant phenotype. Thus, we can use this characteristic to estimate base substitution sites that lead to amber or ochre in the *nprR*-coding region up to at least the point (codon 410) where we have detected a nonsense mutation [TAT (tyr) → TAG (stop)], so that fragments of this length or shorter would not be active. There are 221 such sites. UGA (opal) mutations are also nonsense mutations, but some maybe counteracted by low level natural suppressors so it is not clear how many would show up in the system. Taken together with the 20 detected sites that result in non-amber/ochre mispair, we estimate the *nprR*-coding region has at least 240 potential sites available for analysing base substitution mutations (Table 6). The frequency of obtaining *nprR* mutants among isolated papillation mutants varies from 10% to 50% (data not shown) and therefore makes it both an attractive and a feasible system for analysing mutational specificities.

Experimental procedures

Bacterial strains and growth conditions

A derivative of the wild-type *B. anthracis* Sterne 7702 (pXO1⁺ pXO2⁻, a gift from Dr K. Bradley, University of California, Los Angeles) was used as the parental strain for papillation mutant isolation and *Himar1* minitransposon insertion library construction. *Escherichia coli* strains MACH1 and DH5 α were used for cloning. Unless described elsewhere, cells were cultured in LB broth [10 g l⁻¹ of tryptone (Bacto), 5 g l⁻¹ of yeast extract (Bacto) and 10 g⁻¹ of NaCl (Sigma)] and were supplemented with 15 g l⁻¹ of agar (Bacto) for growth on plates. Antibiotic concentrations used were ampicillin (100 μ g ml⁻¹ for *E. coli*), kanamycin (50 μ g ml⁻¹ for *B. anthracis*), tetracycline (5 μ g ml⁻¹ for *B. anthracis*) and erythromycin (5 μ g ml⁻¹ for *B. anthracis*). The sporulation medium was prepared according to the previously published protocol (Kreuzer-Martin *et al.*, 2003) and was supplemented with

15 g l⁻¹ of agar (Bacto) for plates. The milk plates were prepared essentially the same as the previously published method (Chu, 2007) except 10% non-fat dry milk powder was used in replacing skim milk. *B. anthracis* colonies and cell patches were observed using a dissection microscope. Photographs of the colonies and cell patches were taken using a Leica MZ 10F Stereomicroscope (Leica). Photographs of spores and rod-shaped cells were taken using a Nikon ECLIPSE 80i phase contrast microscope (Nikon). Cells were scraped from the centre or the edge of the cell patch from LB or SM plates at day 6 and smeared on the glass slide. A drop of 5 μ l water was added to the slide and the cell morphology was observed under the Nikon phase contrast microscope.

Papillation mutants

Wild-type *B. anthracis* cells were streaked on LB plates (150 × 15, Fisher) and incubated at 30°C for 6–8 days. Papillae were randomly picked with toothpicks from individual colonies and streaked on LB plates. After a 2 day incubation at 30°C, the colonies that appeared thicker than the surrounding colonies and displayed a different light reflection feature were chosen for further study. A single colony was chosen from each papilla. They were arrayed into 96-well flat-bottom microtiter plates (BD) filled with 0.1 ml BHI plus 0.5% glycerol. After a 1 day incubation at 37°C, 0.1 ml of BHI plus 50% glycerol were added to each well and the plates were stored at –80°C.

To verify the phenotype of a papillation mutant, both the wild type and the mutant were streaked on the same LB plate in a pattern where the colonies overlapped at the centre. After a 2 day incubation at 30°C colonies of the papillation mutant appeared thicker than those of the wild type, had a different light reflection feature, and in many cases had no visible papillae on day 6.

To study cell patch morphology of papillation mutants, the Duetz cryoreplicator was used, allowing simultaneous and reproducible sampling of 96 samples at the same time (Duetz *et al.*, 2000). Using the cryoreplicator, papillation mutants were first transferred from a frozen glycerol plate to a 96 deep-well plate (Fisher) containing 0.5 ml LB. After incubation at 37°C overnight they were transferred simultaneously onto one or several solid agar plates. The plates were incubated at 30°C or 37°C for the period specified in the text.

Himar1 minitransposon insertion library

A shuttle plasmid pUTE583 (a gift from Dr T. M. Koehler, the University of Texas Health Science Center Medical School; Chen *et al.*, 2004), which contains replication origins for both *E. coli* (pUC origin) and *B. anthracis* (pBC16 origin) and their

corresponding antibiotic resistance gene cassettes (Cm^r and Em^r, respectively), was modified to serve as a suicide vector (designated as pSV1) for *B. anthracis* by eliminating the pBC16 origin of replication from the plasmid. The *Himar1* minitransposon from pUTE664 (McGillivray *et al.*, 2009) that contains a kanamycin resistance gene cassette flanking with short ITRs, together with its corresponding transposase gene (outside of ITRs) was introduced into pSV1 to make a *Himar1* minitransposon suicide delivery vector designated as pSV2.

To mutagenize *B. anthracis*, pSV2 prepared from an *E. coli* strain GM2163 lacking DNA methylation modification systems, was introduced into *B. anthracis* by electroporation. We modified an established electroporation protocol (Koehler *et al.*, 1994) with a protocol for preparing *E. coli* competent cells (MicroPulser Electroporation Apparatus Operating Instructions, BIO-RAD). Briefly, a culture containing 250 ml of freshly grown *B. anthracis* with OD₆₀₀ of 0.6–0.8 was washed three times in ice-cold 10% glycerol by centrifugation and resuspended in ice-cold 10% glycerol to a final volume of 0.8–1 ml. At this point, the cell suspension had a consistency of a viscous off-white paste and the cells were ready for electroporation. DNA (pSV2, 16 µg) was added to 0.2 ml cell suspension. After the cells came in contact with the DNA for about 1 min an electric pulse was delivered using GENE PULSER II (BIO-RAD). Immediately after the pulse, the cells were recovered in 20 ml BGGM (BHI plus 10% glycerol, 0.4% glucose and 10 mM MgCl₂) in a 500 ml flask with vigorous shaking at 37°C for 30 to 60 min. The cells were collected by centrifugation at 4°C and were plated onto the selective LB antibiotic plates containing Kanamycin (50 µg ml⁻¹). After 1 day incubation at room temperature (~23°C) and 1 day incubation at 30°C, individual kanamycin resistant colonies were arrayed into 96-well flat bottom plates (BD) and stored at -80°C for further analysis.

The following three aspects were analysed: donor plasmid integration, insertion site identification and verification. The antibiotic resistance marker (Em^r) on the backbone of the donor plasmid pSV2 was used to estimate the percentage of the donor plasmid integration among the transposon-insertion mutants. We found that 98.5% transformants were free of the delivery plasmid backbone among 2200 transposon-insertion mutants analysed. We adapted an efficient, semirandom, PCR-based high-throughput method (Gallagher *et al.*, 2007; Cameron *et al.*, 2008) for identifying and verifying transposon insertion sites with an average success rate of 89% among 337 mutants sequenced. The primer sequences can be obtained upon request. We further verified the insertion sites on eight mutants using a different set of transposon PCR and sequencing primers located at the opposite end of the original mapping primers. All eight insertion sites identified from the second set of primers matched perfectly to those obtained from the first mapping.

Detection of *nprR* mutations

To prepare DNA samples from papillation mutants, 10 µl of the supernatant was collected from a small amount of cells after boiling for 10 min in 20 µl of water by centrifugation. A DNA fragment containing the *nprR* gene was amplified and sequenced using previously published protocols (PCR round 2/cleanup/sequencing; Gallagher *et al.*, 2007). The PCR

primers are BAS0566A 5'-AGCGGCGATTGTGAATACC-3' (300 bp immediately upstream of *nprR*) and BAS0566B 5'-GAGCACATTTTTAGAACTGCA-3' (400 bp immediately downstream of *nprR*). The sequencing primers are BAS0566A and BAS0566D 5'-GTAATGGCCAAGGAAC AAGGT-3'. The sequences obtained from the samples were compared with the wild-type *nprR* sequence obtained from the database using Seqman (DNASTAR).

Mutator screening

To search for mutators that carry elevated levels of papillation we screened transposon-insertion mutants grown on the transposon selection plates for 5 to 6 days at 30°C. The levels of papillation for each colony were observed and compared under a dissection microscope. The colonies that displayed elevated levels of papillation were picked and streaked on LB plates. After a 2 day incubation at 30°C, several single colonies that had the normal light reflection feature (avoiding papillation mutants) were chosen to be arrayed in a 96-well plate along with a wild-type control. To verify the mutator phenotype, these isolates were printed onto an LB plate via Duetz cryoreplicator and incubated at 30°C for 6 days. The levels of papillation of these isolates were compared with the wild-type control arrayed on the same plate. We also screened the transposon-insertion mutants (~2000) that were already arrayed in the 96-well plates after 2 day incubation on the transposon selection plates. The transposon-insertion sites of the candidates were mapped according to the protocols described in the section '*Himar1* minitransposon insertion library'.

rpoB/Rif^r and *nprR*/papillation systems

The mutational frequency in the *rpoB* gene that leads to the Rif^r phenotype was measured using previously published protocols (Vogler *et al.*, 2002; Zeibell *et al.*, 2007). The procedures used for the detection of Rif^r mutants and determination of the base substitution spectrum in the *rpoB* gene were as previously published (Vogler *et al.*, 2002; Zeibell *et al.*, 2007). The procedures for identification of group A papillation mutants are described in the text. Briefly, the group A papillation mutants were sorted out from the papillation mutant collection by their cell patch morphology on LB, sporulation and milk plates. The determination of the mutational spectrum in the *nprR* gene was according to the protocols described in the section '*Detection of nprR mutations*'.

Complementation using the wild-type *nprR* and *ycyJ* genes

A DNA fragment containing the wild-type *nprR* gene was amplified using PCR and cloned into the PCR2.1-TOPO vector (Invitrogen) using TOPO TA cloning kit (Invitrogen). The PCR primers are BAS0566A and BAS0566G 5'-TC TTTTTCATTTTTATTCTCCTT-3' (12 bp immediately downstream of *nprR*). The fragment containing the wild-type *nprR* gene was subcloned into the shuttle vector pUTE29 (Koehler

et al., 1994; McGillivray et al., 2009). The pUTE29nprR plasmid (prepared from a methylation deficient *E. coli* strain GM2163) was electroporated into two mutants, T13B11 (Table 1, No. 39) and T13G5 (Table 1, No. 19), as well as a wild type. The vector pUTE29 was also included in the experiment as a negative control. The transformants were selected on the LB plates containing 5 µg ml⁻¹ tetracycline. A drop of an overnight culture of each strain was placed on the milk plates to observe extracellular protease production (37°C overnight).

DNA fragments containing the intergenic region located immediately upstream of the *walkR* operon and the coding region of the *yycJ* gene were amplified using PCR and cloned into the PCR2.1-TOPO vector (Invitrogen) using TOPO TA cloning kit (Invitrogen) respectively. The primers for amplifying the intergenic region are YYCJ3 5'-CTCAGGATATTAAGTGGGCC-3' (401 bp immediately upstream of *walkR*) and YYCJ4 5'-CTGTGCGACCATCATCGTCTATTTCTCCTTA-3' (17 bp immediately before the *walkR* gene plus ATGATG and a Sall site). The primers for amplifying the coding region of *yycJ* are YYCJ5 5'-CAGGATCCGGGTTGCATTTAGTG TACTTG-3' (a Sall site plus 22 bp immediately downstream of the start codon ATG) and YYCJ6 5'-CTGTGCGACATATTGTTACCTATCTTCTG-3' (66 bp immediately downstream of *yycJ*). These two fragments were fused at the Sall site to form the fusion *yycJ1* (Fig. 4C) and the fusion was subcloned into the shuttle vector pUTE29 (Koehler et al., 1994; McGillivray et al., 2009). The pUTE29 vector alone was also included in the experiment as a negative control. Both pUTE29yycJ1 and pUTE29 were prepared from a methylation deficient *E. coli* strain GM2163 and electroporated into the mutant *yycJ*, *yycH yycI* and the wild type; and the transformants were selected on the LB plates containing 5 µg ml⁻¹ tetracycline. The transformants were streaked on the LB plates containing 5 µg ml⁻¹ tetracycline and incubated at 30°C for 6 days to observe papillation.

Construction of a *recJ* mutant via a suicide vector mediated gene allele exchange

The *recJ* coding region contains 2340 bp. A DNA fragment containing a partial *recJ* coding region was amplified using PCR and cloned into the PCR2.1-TOPO vector (Invitrogen) using TOPO TA cloning kit (Invitrogen). The PCR primers are RecJ3 (5'-ATTACAGATCACCATGAGCCG-3', 496 bp from the start codon) and RecJ13 (5'-GCAATACTACGCGCTGAACC-3', 1165 bp from the start codon). The partial *recJ* fragment was subcloned into the suicide vector pSV1, electroporated into the wild-type *B. anthracis* competent cells (prepared using the same protocol as described in *Himar1* minitransposon insertion library) and plated onto LB plates with 10 µg ml⁻¹ erythromycin. After 1 day incubation at 37°C and 1 day at room temperature, the Em^r colonies were picked and isolated on LB plates with 10 µg ml⁻¹ erythromycin. Disruption of the *recJ* coding region in the Em^r mutants was verified by PCR using the following primer sets: RecJ3/RecJ4 (5'-GCCATGCCTCTACAGCAATATC-3') and RecJ4/RecJ1 (5'-ATCGCATTGGAAAGCATGTG-3'). The determination of the mutational spectrum in the *nprR* gene was according to the protocols described in the section 'Detection of *nprR* mutations'.

Acknowledgements

We are grateful to Ken Bradley, Wei Yang and Paul Keim for helpful advice. We thank Wenyan Shi for providing Leica MZ 10F Stereomicroscope, Nikon phase contrast microscope and technical support. This work was supported by a grant from the National Institutes of Health (ES0110875). S.M.M. was supported by an NIH IRACDA postdoctoral fellowship (GM068524) and a Biomedical Research Fellowship from The Hartwell Foundation.

References

- Bergman, N.H., Anderson, E.C., Swenson, E.E., Niemeyer, M.M., Miyoshi, A.D., and Hanna, P.C. (2006) Transcriptional profiling of the *Bacillus anthracis* life cycle *in vitro* and an implied model for regulation of spore formation. *J Bacteriol* **188**: 6092–6100.
- Bongiorni, C., Stoessel, R., and Perego, M. (2007) Negative regulation of *Bacillus anthracis* sporulation by the Spo0E family of phosphatases. *J Bacteriol* **189**: 2637–2645.
- Cabrera, M., Nghiem, Y., and Miller, J.H. (1988) *mutM*, a second mutator locus in *Escherichia coli* that generates G.C → T.A transversions. *J Bacteriol* **170**: 5405–5407.
- Cameron, D.E., Urbach, J.M., and Mekalanos, J.J. (2008) A defined transposon mutant library and its use in identifying motility genes in *Vibrio cholerae*. *Proc Natl Acad Sci USA* **105**: 8736–8741.
- Chen, Y., Tenover, F.C., and Koehler, T.M. (2004) Beta-lactamase gene expression in a penicillin-resistant *Bacillus anthracis* strain. *Antimicrob Agents Chemother* **48**: 4873–4877.
- Chu, W.-H. (2007) Optimization of extracellular alkaline protease production from species of *Bacillus*. *J Ind Microbiol Biotechnol* **34**: 241–245.
- Cupples, C.G., and Miller, J.H. (1989) A set of *lacZ* mutations in *Escherichia coli* that allow rapid detection of each of the six base substitutions. *Proc Natl Acad Sci USA* **86**: 5345–5349.
- Cupples, C.G., Cabrera, M., Cruz, C., and Miller, J.H. (1990) A set of *lacZ* mutations in *Escherichia coli* that allow rapid detection of specific frameshift mutations. *Genetics* **125**: 275–280.
- Day, W.A., Jr, Rasmussen, S.L., Carpenter, B.M., Peterson, S.N., and Friedlander, A.M. (2007) Microarray analysis of transposon insertion mutations in *Bacillus anthracis*: global identification of genes required for sporulation and germination. *J Bacteriol* **189**: 3296–3301.
- Dean, A.C.R., and Hinshelwood, C. (1957a) The formation of papillae on bacterial colonies. I. *Proc R Soc Lond B Biol Sci* **147**: 1–9.
- Dean, A.C.R., and Hinshelwood, C. (1957b) The formation of papillae on bacterial colonies. II. *Proc R Soc Lond B Biol Sci* **147**: 10–20.
- Declerck, N., Bouillaut, L., Chaix, D., Rugani, N., Slamti, L., Hoh, F., et al. (2007) Structure of PlcR: insights into virulence regulation and evolution of quorum sensing in Gram-positive bacteria. *Proc Natl Acad Sci USA* **104**: 18490–18495.
- Dixon, W.J., and Massey, F.J., Jr (1969) *Introduction to Statistical Analysis*. New York, NY: McGraw-Hill.

- Dominski, Z. (2007) Nucleases of the metallo-beta-lactamase family and their role in DNA and RNA metabolism. *Crit Rev Biochem Mol Biol* **42**: 67–93.
- Dubrac, S., Bisicchia, P., Devine, K.M., and Msadek, T. (2008) A matter of life and death: cell wall homeostasis and the WalkR (YycG) essential signal transduction pathway. *Mol Microbiol* **70**: 1307–1322.
- Duetz, W.A., Rüedi, L., Hermann, R., O'Connor, K., Büchs, J., and Witholt, B. (2000) Methods for intense aeration, growth, storage, and replication of bacterial strains in microtiter plates. *Appl Environ Microbiol* **66**: 2641–2646.
- Dutra, B.E., Sutura, V.A., Jr, and Lovett, S.T. (2007) RecA-independent recombination is efficient but limited by exonucleases. *Proc Natl Acad Sci USA* **104**: 216–221.
- Farabaugh, P.J., Schmeissner, U., Hofer, M., and Miller, J.H. (1978) Genetic studies of the *lac* repressor. VII. On the molecular nature of spontaneous hotspots in the *lacI* gene of *Escherichia coli*. *J Mol Biol* **126**: 847–857.
- Feschenko, V.V., Rajman, L.A., and Lovett, S.T. (2003) Stabilization of perfect and imperfect tandem repeats by single-strand DNA exonucleases. *Proc Natl Acad Sci USA* **100**: 1134–1139.
- Foster, P.L. (1993) Adaptive mutation: the uses of adversity. *Annu Rev Microbiol* **47**: 467–504.
- Foster, P.L. (2007) Stress-induced mutagenesis in bacteria. *Crit Rev Biochem Mol Biol* **42**: 373–397.
- Fukushima, T., Szurmant, H., Kim, E.J., Perego, M., and Hoch, J.A. (2008) A sensor histidine kinase co-ordinates cell wall architecture with cell division in *Bacillus subtilis*. *Mol Microbiol* **69**: 621–632.
- Gallagher, L., Turner, C., Ramage, E., and Manoil, C. (2007) Creating recombination-activated genes and sequence-defined mutant libraries using transposons. *Methods Enzymol* **421**: 126–140.
- Han, E.S., Cooper, D.L., Persky, N.S., Sutura, V.A., Jr, Whittaker, R.D., Montello, M.L., and Lovett, S.T. (2006) RecJ exonuclease: substrates, products and interaction with SSB. *Nucleic Acids Res* **34**: 1084–1091.
- Koehler, T.M. (2009) *Bacillus anthracis* physiology and genetics. *Mol Aspects Med* **30**: 386–396.
- Koehler, T.M., Dai, Z., and Kaufman-Yarbray, M. (1994) Regulation of the *Bacillus anthracis* protective antigen gene: CO₂ and a trans-acting element activate transcription from one of two promoters. *J Bacteriol* **176**: 586–595.
- Kolstø, A.B., Tourasse, N.J., and Økstad, O.A. (2009) What sets *Bacillus anthracis* apart from other *Bacillus* species? *Annu Rev Microbiol* **63**: 451–476.
- Konrad, E.B. (1977) Method for the isolation of *Escherichia coli* mutants with enhanced recombination between chromosomal duplications. *J Bacteriol* **130**: 167–172.
- Kreuzer-Martin, H.W., Lott, M.J., Dorigan, J., and Ehleringer, J.R. (2003) Microbe forensics: oxygen and hydrogen stable isotope ratios in *Bacillus subtilis* cells and spores. *Proc Natl Acad Sci USA* **100**: 815–819.
- Kroos, L. (2007) The *Bacillus* and *Myxococcus* developmental networks and their transcriptional regulators. *Annu Rev Genet* **41**: 13–39.
- Kumar, G.A., Woodhall, M.R., Hood, D.W., Moxon, E.R., and Bayliss, C.D. (2008) RecJ, ExoI and RecG are required for genome maintenance but not for generation of genetic diversity by repeat-mediated phase variation in *Haemophilus influenzae*. *Mutat Res* **640**: 46–53.
- Lacks, S., and Greenberg, B. (1977) Competence for deoxyribonucleic acid uptake and deoxyribonuclease action external to cells in the genetic transformation of *Diplococcus pneumoniae*. *J Bacteriol* **114**: 152–163.
- Lampe, D.J., Akerley, B.J., Rubin, E.J., Mekalanos, J.J., and Robertson, H.M. (1999) Hyperactive transposase mutants of the *Himar1* mariner transposon. *Proc Natl Acad Sci USA* **96**: 11428–11433.
- Massini, R. (1907) Über einen in biologischer Beziehung interessanten Kolistamm (*Bacterium coli mutabile*). *Arch f Hyg* **61**: 250–292.
- McGillivray, S.M., Ebrahimi, C.M., Fisher, N., Sabet, M., Zhang, D.X., Chen, Y., et al. (2009) ClpX contributes to innate defense peptide resistance and virulence phenotypes of *Bacillus anthracis*. *J Innate Immun* **1**: 494–506.
- Michaels, M.L., Cruz, C., and Miller, J.H. (1990) *mutA* and *mutC*: two mutator loci in *Escherichia coli* that stimulate transversions. *Proc Natl Acad Sci USA* **87**: 9211–9215.
- Miller, J.H. (1996) The relevance of bacterial mutators to understanding human cancer. *Cancer Surv* **28**: 141–153.
- Miller, J.H., and Albertini, A.M. (1983) Effects of surrounding sequence on the suppression of nonsense codons. *J Mol Biol* **164**: 59–71.
- Miller, J.H., and Michaels, M. (1996) Finding new mutator strains of *Escherichia coli* – a review. *Gene* **179**: 129–132.
- Miller, J.H., Funchain, P., Clendenin, W., Huang, T., Nguyen, A., Wolff, E., et al. (2002) *Escherichia coli* strains (*ndk*) lacking nucleoside diphosphate kinase are powerful mutators for base substitutions and frameshifts in mismatch-repair-deficient strains. *Genetics* **162**: 5–13.
- Monod, J., and Audureau, A. (1946) Mutation et adaptation enzymatique chez *Escherichia coli-mutabile*. *Annales de l'Institut Pasteur* **72**: 868–878.
- Ng, W.L., Robertson, G.T., Kazmierczak, K.M., Zhao, J., Gilmour, R., and Winkler, M.E. (2003) Constitutive expression of PcsB suppresses the requirement for the essential VicR (YycF) response regulator in *Streptococcus pneumoniae* R6. *Mol Microbiol* **50**: 1647–1663.
- Nghiem, Y., Cabrera, M., Cupples, C.G., and Miller, J.H. (1988) The *mutY* gene: a mutator locus in *Escherichia coli* that generates G.C → T.A transversions. *Proc Natl Acad Sci USA* **85**: 2709–2713.
- Ohlsen, K.L., Grimsley, J.K., and Hoch, J.A. (1994) Deactivation of the sporulation transcription factor Spo0A by the Spo0E protein phosphatase. *Proc Natl Acad Sci USA* **91**: 1756–1760.
- Parr, L.W., and Thomas, H. (1942) Search for paracolon in *Bacterium Coli-Mutable* populations. *J Hered* **33**: 93–96.
- Perego, M., and Hoch, J.A. (1991) Negative regulation of *Bacillus subtilis* sporulation by the *spo0E* gene product. *J Bacteriol* **173**: 2514–2520.
- Perego, M., and Hoch, J.A. (2002) Two-component systems, phosphorelays, and regulation of their activities by phosphatases. In *Bacillus Subtilis and its Closest Relatives: from Genes to Cells*. Sonenshein, A.L., Hoch, J.A., and Losick, R. (eds). Washington, DC: ASM press, pp. 473–481.
- Perego, M., Hanstein, C., Welsh, K.M., Djavakhishvili, T., Glaser, P., and Hoch, J.A. (1994) Multiple protein-aspartate

- phosphatases provide a mechanism for the integration of diverse signals in the control of development in *B. subtilis*. *Cell* **79**: 1047–1055.
- Pottathil, M., and Lazazzera, B.A. (2003) The extracellular Phr peptide-Rap phosphatase signaling circuit of *Bacillus subtilis*. *Front Biosci* **8**: d32–d45.
- Robledo, E.A., Yasbin, R., Ross, C., and Pedraza-Reyes, M. (2007) Stationary phase mutagenesis in *B. subtilis*: a paradigm to study genetic diversity programs in cells under stress. *Crit Rev Biochem Mol Biol* **42**: 327–339.
- Rocha-Estrada, J., Aceves-Diez, A.E., Guarneros, G., and de la Torre, M. (2010) The RNPP family of quorum-sensing proteins in Gram-positive bacteria. *Appl Microbiol Biotechnol* **87**: 913–923.
- Senadheera, M.D., Lee, A.W., Hung, D.C., Spatafora, G.A., Goodman, S.D., and Cvitkovitch, D.G. (2007) The *Streptococcus mutans vicX* gene product modulates *gtfB/C* expression, biofilm formation, genetic competence, and oxidative stress tolerance. *J Bacteriol* **189**: 1451–1458.
- Slupska, M.M., Chiang, J.H., Luther, W.M., Stewart, J.L., Amii, L., Conrad, A., and Miller, J.H. (2000) Genes involved in the determination of the rate of inversions at short inverted repeats. *Genes Cells* **5**: 425–437.
- Spiegelman, G., Van Hoy, B., Perego, M., Day, J., Trach, K., and Hoch, J.A. (1990) Structural alterations in the *Bacillus subtilis* Spo0A regulatory protein which suppress mutations at several *spo0* loci. *J Bacteriol* **172**: 5011–5019.
- Stewart, F.H. (1928) The life-cycle of bacteria. Alternate asexual and autogamic phases. *J Hyg (Lond)* **27**: 379–395.
- Szurmant, H., Fukushima, T., and Hoch, J.A. (2007a) The essential YycFG two-component system of *Bacillus subtilis*. *Methods Enzymol* **422**: 396–3417.
- Szurmant, H., Mohan, M.A., Imus, P.M., and Hoch, J.A. (2007b) YycH and YycI interact to regulate the essential YycFG two-component system in *Bacillus subtilis*. *J Bacteriol* **189**: 3280–3289.
- Szurmant, H., Bu, L., Brooks, C.L., 3rd, and Hoch, J.A. (2008) An essential sensor histidine kinase controlled by trans-membrane helix interactions with its auxiliary proteins. *Proc Natl Acad Sci USA* **105**: 5891–5896.
- Viswanathan, M., Burdett, V., Baitinger, C., Modrich, P., and Lovett, S.T. (2001) Redundant exonuclease involvement in *Escherichia coli* methyl-directed mismatch repair. *J Biol Chem* **276**: 31053–33108.
- Vogler, A.J., Busch, J.D., Percy-Fine, S., Tipton-Hunton, C., Smith, K.L., and Keim, P. (2002) Molecular analysis of rifampin resistance in *Bacillus anthracis* and *Bacillus cereus*. *Antimicrob Agents Chemother* **46**: 511–513.
- Wang, M., Yang, Z., Rada, C., and Neuberger, M.S. (2009) AID upmutants isolated using a high-throughput screen highlight the immunity/cancer balance limiting DNA deaminase activity. *Nat Struct Mol Biol* **16**: 769–776.
- Whoriskey, S.K., Nghiem, V.H., Leong, P.M., Masson, J.M., and Miller, J.H. (1987) Genetic rearrangements and gene amplification in *Escherichia coli*: DNA sequences at the junctures of amplified gene fusions. *Genes Dev* **1**: 227–237.
- Yabuuchi, E., and Koseki, M. (2003) Morphology of the type strain of *Bacillus anthracis* EY 3169^T = ATCC 14578^T grown either aerobically or anaerobically on agar plates – observation by light and laser microscopes. *Microbiol Immunol* **47**: 491–497.
- Zeibell, K., Aguila, S., Shi, V.Y., Chan, A., Yang, H., and Miller, J.H. (2007) Mutagenesis and repair in *Bacillus anthracis*: the effect of mutators. *J Bacteriol* **189**: 2331–2338. Erratum in: *J Bacteriol* 189: 3932.